doi:10.1093/jmcb/mjz031
Published online May 8, 2019

Article

Loss of mismatch repair signaling impairs the WNT–bone morphogenetic protein crosstalk and the colonic homeostasis

Katrine Nørgaard[1], Carolin Müller[1], Nadja Christensen[1], María L. Chiloeches[1], Cesilie L. Madsen[1], Sabine S. Nielsen[1], Tine E. Thingholm[1,2], and Antoaneta Belcheva[1,*]

[1] Department of Biochemistry and Molecular Biology, University of Southern Denmark, Campusvej 55, 5230 Odense M, Denmark
[2] Department of Molecular Medicine, University of Southern Denmark, J.B. Winsløws Vej 25, 5230 Odense M, Denmark
* Correspondence to: Antoaneta Belcheva, E-mail: belcheva@bmb.sdu.dk

Edited by Zhiyuan Shen

The fine balance between proliferation, differentiation, and apoptosis in the colonic epithelium is tightly controlled by the interplay between WNT, Notch, and bone morphogenetic protein (BMP) signaling. How these complex networks coordinate the colonic homeostasis, especially if cancer predisposing mutations such as mutations in the DNA mismatch repair (MMR) are present, is unclear. Inactivation of the MMR system has long been linked to colorectal cancer; however, little is known about its role in the regulation of the colonic homeostasis. It has been shown that loss of MMR promotes the proliferation of colon epithelial cells that renders them highly susceptible to transformation. The mechanism through which MMR mediates this effect, yet, remains to be determined. Using an MMR-deficient mouse model, we show that increased methylation of Dickkopf1 impacts its expression, and consequently, the ability to negatively regulate WNT signaling. As a result, excessive levels of active β-catenin promote strong crypt progenitor-like phenotype and abnormal proliferation. Under these settings, the development and function of the goblet cells are affected. MMR-deficient mice have fewer goblet cells with enlarged mucin-loaded vesicles. We further show that MMR inactivation impacts the WNT–BMP signaling crosstalk.

Keywords: MMR, colonic epithelium, WNT, BMP, crypt homeostasis

Introduction

The DNA mismatch repair (MMR) is a highly conserved DNA repair system that plays a central role in maintaining the genomic stability of the cells. The MMR proteins recognize DNA single-base mutations and small insertion or deletion loops, generated during DNA replication, and coordinate their repair. Initially, the DNA damage is recognized by the protein MutS homologue 2 (Msh2) that forms a complex with one of its partner proteins Msh6 or Msh3 depending on the type of DNA damage (Jiricny, 2006). Msh2 then recruits other downstream components of the pathway that excise and resynthesize the damaged DNA region. Therefore, Msh2 is a key MMR protein, and its inactivation completely abolishes the DNA repair process (Modrich and Lahue, 1996; Jiricny, 2006). Loss of MMR activity is associated with both hereditary and sporadic colorectal cancer (CRC) (Ionov et al., 1993; Marra and Jiricny, 2005; Poulogiannis et al., 2010). One of the hallmarks of MMR deficiency is the development of mutator phenotype seen as elevated frequency of single-base substitutions and small insertion/deletion mismatches that are generated at repeated DNA sequences, known also as microsatellite instability (MSI). Indeed, MSI is recognized as the main mechanism through which MMR deficiency mediates CRC initiation, nicely reviewed by Boland and Goel (2010). MMR pathway also plays a critical role in initiation of apoptosis in response to high levels of DNA damage. Therefore, failure to trigger apoptosis was recognized as another mechanism through which MMR deficiency contributes to CRC (Negureanu and Salsbury, 2012; Li et al., 2016). Interestingly, inactivation of MMR pathway increases susceptibility to carcinogenesis of particular types of cells. The most susceptible tissue is the colonic epithelium, followed by endometrium, stomach, kidney, ovary, and small intestine (Chao and Lipkin, 2006). Significantly lower risk for cancer incidence is reported in prostate, breast, and lung tissues (Watson and Lynch, 2001). Studies with MMR mutant mouse models have further provided significant knowledge about the

Received August 22, 2018. Revised December 14, 2018. Accepted March 17, 2019.

mechanisms of cancer susceptibility in different types of tissue (Heyer et al., 1999; Lee et al., 2016). It has been suggested that high proliferation rate, as well as rapid acceleration/deceleration of the proliferation rate, plays a critical role in the process of cell transformation (Chao and Lipkin, 2006).

Since its discovery, extensive research has been focused on revealing the molecular mechanisms through which MMR deficiency mediates tumor development. In contrast, very little is known about the role of MMR pathway in the regulation of the colonic homeostasis. The colon epithelial cells (CECs) are organized in colonic crypts. The colonic crypt itself is composed by stem cells that are located at the bottom of the crypt, which proliferate and give rise to their daughter cells known as transit-amplifying cells (TA cells). The stem cells and TA cells form the so-called proliferative compartment of the crypt. As these cells proliferate, they also move upwards toward the intestinal lumen where they differentiate into goblet cells, enterocytes, and enteroendocrine cells (Medema and Vermeulen, 2011). Three signaling pathways tightly regulate the proliferation and differentiation of the CECs: WNT/β-catenin, Notch, and bone morphogenetic protein (BMP) pathways. It is generally accepted that WNT regulates the proliferation of the CECs. The myofibroblast cells at the bottom of the colonic crypts produce several WNT ligands, so that the stem cells and TA cells are exposed to higher amounts of WNT molecules. Typically, the WNT ligands interact with their receptors and activate signaling cascades that result in disassembling of the β-catenin destruction complex, which involves adenomatous polyposis coli (APC), axis inhibition protein 2 (Axin2), casein kinase 1, and glycogen synthase kinase-3β (GSK-3β). This further leads to stabilization and accumulation of non-phosphorylated (active) β-catenin. Activated β-catenin then enters the nucleus and together with its co-factors mediates the transcription of genes that are required to maintain the proliferation of the cells (Medema and Vermeulen, 2011). The myofibroblast cells also secrete several BMP ligands. However, the signaling molecule Noggin effectively inhibits their activity at the bottom of the colonic crypts. The Noggin concentration gradually decreases toward the intestinal lumen so that BMP ligands gain their activity and interact with BMPR1 and BMPR2 receptors, resulting in phosphorylation of Smad1/5/8 and its cooperation with Smad4. Subsequently, the formed Smad complex transcribes genes that regulate cell cycle arrest, differentiation, or apoptosis of the CECs (Medema and Vermeulen, 2011). On the other hand, Notch regulates the equilibrium between cell proliferation and differentiation by directing the response of the cells to specific environmental signals (Artavanis-Tsakonas et al., 1999). Notch 1 and Notch 2 receptors, their specific ligands Jagged 1 (Jag1), Delta-like 1 (Dll1), and Dll4, and the Notch target genes hairy and enhancer of split 1 (*Hes1*), *Hes5*, and *Hes6* are highly active in the proliferative compartment of the colonic crypts and are important for the maintenance of the colonic stem cell niche (Jensen et al., 2000; Schroder and Gossler, 2002; VanDussen et al., 2012). A great amount of research has focused on elucidation of the specific roles of WNT, BMP, and Notch signaling in the regulation of proliferation and differentiation of CECs. However, our knowledge of how these pathways crosstalk with each other to maintain the normal colonic homeostasis is still very limited. Moreover, how this crosstalk is impacted by specific genetic mutations that predispose to cancer is unclear.

It has been shown that inactivation of MMR system in mice results in increased proliferation of CECs that renders these cells highly susceptible to transformation events (Belcheva et al., 2014). Although it has been suggested that this phenomenon is caused by elevated WNT/β-catenin signaling, the mechanistic links were not elucidated.

Here we investigated the causative factors leading to overactivation of WNT signaling pathway in Msh2-deficient CECs and its impact on the colonic homeostasis. We found that WNT functions normally upstream of the β-catenin destruction complex and the presence of excessive active form of the protein is caused by loss of expression of the WNT inhibitor Dickkopf1 (DKK1). Our data show that increased methylation of *DKK1* CpG island in $Msh2^{-/-}$ CECs is a mechanism for its downregulation. As a result, the activated β-catenin promotes strong crypt progenitor-like phenotype and enhanced proliferation. Under these settings, the normal development and function of the goblet cells are affected. We observed significant reduction in the goblet cell numbers, which, however, produce substantially more Mucin 2 (Muc2). We also show that failure to regulate β-catenin activity in Msh2-deficient CECs has an impact on the molecular crosstalk between WNT and BMP signaling pathways.

Results

Inactivation of MMR pathway is associated with strong stem cell-like phenotype

The CECs are organized in colonic crypts where the proliferating cells (stem cells and their daughter progenitor cells) and terminally differentiated cells (enterocytes, enteroendocrine, and goblet cells) are maintained in precisely controlled homeostasis (Figure 1A). Mutation in *Msh2* gene results in an increase in the proliferating compartment of the intestinal crypts (Belcheva et al., 2014), also observed in this study (Supplementary Figure S1). This suggests that the normal homeostatic balance between proliferating and differentiated cells is likely impacted by the *Msh2* mutation. To investigate this hypothesis, we analyzed the expression of several stem cell and differentiated cell markers in colonic crypts derived from $Msh2^{-/-}$ mice and their WT controls ($Msh2^{+/-}$ mice). Previously reported significant increase in Ephrin type-B receptor 2 (*EphB2*), *EphB3*, and *CD44* mRNA levels in $Msh2^{-/-}$ colonic crypts (Belcheva et al., 2014) was also confirmed in this study (Figure 1B; Supplementary Figure S2). In addition, the stem cell marker Achaete-scute-like 2 (*Ascl2*), a gene with pivotal role in defining the stem cell identity (Schuijers et al., 2015), was also significantly elevated (Figure 1B). Although not significant, the expression of the stem cell marker *CD24* was increased by 1.5-fold in $Msh2^{-/-}$ CECs (Figure 1B). The increased *EphB2* mRNA levels in Msh2 mutant CECs also correlated with notably higher protein abundance (Figure 1C). In addition, the typical EphB2 expression gradient pattern was

altered in Msh2-deficient crypts. We observed extensive EphB2 expression at the bottom of the colonic crypts and prolonged decreasing gradient compared to WT controls (Figure 1C). EphB2 expression pattern is critical for establishment of balanced distribution of proliferating and differentiated cells within the colonic crypt (Batlle et al., 2002) and together with EphB3, CD44, Ascl2, and CD24 are direct transcriptional targets of WNT/β-catenin signaling (Pinto et al., 2003; Schuijers et al., 2015). To further understand whether these stem cell markers were increased in Msh2 mutant CECs due to alterations in WNT activity, we carried out western blot analysis of β-catenin (Figure 1D). We measured higher expression of the active form of β-catenin (non-phosphorylated β-catenin) in Msh2$^{-/-}$ colonic crypts. This was concomitant with marked decrease in the expression of the negative cell cycle regulator p21$^{CIP1/WAF1}$. Since the reduced p21 expression in Msh2$^{-/-}$ CECs is likely associated with the enhanced proliferation of these cells, we further investigated the mechanism responsible for its negative regulation. p21 transcription is controlled by both p53 (Gartel and Tyner, 1999) and β-catenin (p53-independent mechanism) (Kamei et al., 2003). Specifically, p53^{Ser15} phosphorylation is required for p53 transcriptional activity at the p53-responsive promoters, including the p21 promoter (Loughery et al., 2014). Therefore, we assessed the p53^{Ser15} levels by western blot. The result showed that phospho-p53^{Ser15} levels were not different between Msh2$^{-/-}$ and Msh2$^{+/-}$ cells (Figure 1D), suggesting that the reduced expression of p21 results from the elevated β-catenin activity. Taken together, these results indicate that in Msh2 mutant CECs enhanced β-catenin activity promotes crypt progenitor-like phenotype and enhanced proliferation.

Msh2 mutation impacts the regulation of WNT signaling via DKK1

The activity of β-catenin is controlled by its phosphorylation status. Typically, in the absence of WNT signal, activated GSK-3β plays a central role in phosphorylation of β-catenin, an event that triggers its degradation and shuts down the transcription of β-catenin-regulated genes (Medema and Vermeulen, 2011). Since we measured excessive levels of active β-catenin and marked increase in several stem cell markers in Msh2 mutant colonic crypts, we hypothesized that this may be due to alteration in the GSK-3β activity. However, we found that the active form of the kinase (p-GSK-3β) that is detected by the specific phosphorylation on Tyr216 was not different between Msh2 mutant and Msh2 WT CECs (Figure 2A). Next, we tested the mRNA levels of *APC* and *Axin2*, important components of the β-catenin destruction complex (Medema and Vermeulen, 2011) and are frequent mutational targets of MMR deficiency (Castiglia et al., 2008). The results showed that these genes were not differentially expressed between Msh2 WT and Msh2$^{-/-}$ mice (Figure 2B), suggesting that the increased active β-catenin levels in Msh2 mutant CECs are neither caused by discrete external stimuli that would alter the activity of GSK-3β (Figure 2A), nor by loss of *APC* and *Axin2* expression (Figure 2B). To explain the abundance of the active β-catenin in Msh2 mutant CECs, we further hypothesized that it may be caused by aberrant negative regulation of WNT signaling, mediated by DKK1 protein. DKK1 is a natural WNT antagonist that plays a critical role in the precise regulation of WNT signal transmissions, and therefore, prevents abnormal signaling output (Niida et al., 2004; Gonzlez-Sancho et al., 2005).

Our analysis revealed that the expression of *DKK1* was reduced at both mRNA (Figure 2B) and protein (Figure 2C) levels in Msh2$^{-/-}$ CECs. Indeed, *DKK1* expression is often reduced in CRC (Gonzlez-Sancho et al., 2005). This may be due to mutations in *DKK1* or transcriptional inactivation of *DKK1* via hypermethylation of CpG regions (Aguilera et al., 2006; Sato et al., 2007), a process highly associated with MSI and MMR (Rawson et al., 2011).

To assess whether *DKK1* inactivation is caused by specific mutation(s), genomic DNA was isolated from CECs of four Msh2$^{-/-}$ and three Msh2$^{+/-}$ mice; the entire gene was amplified and subjected to sequencing analysis. The results showed no mutations (not shown).

DKK1 has two CpG islands. The first spans around its transcription start site and the second is located ~600 bp downstream. The location of the predicted CpG islands, the *DKK1* transcription start site, and the location of the primers are shown (Figure 1D). To investigate the methylation state of *DKK1*, we examined the CpG islands by methylation-specific polymerase chain reaction (PCR). We used methBLAST algorithm to design primers that are specific to the bisulfite converted genomic DNA (Pattyn et al., 2006). We were only able to amplify one of the CpG regions. The specificity of the selected primers was evaluated by 1.5% agarose gels. The purified PCR products were sequenced, and the DNA methylation status was determined by comparing the sequencing results with the original DNA sequence. Only presence of a single C-peak that indicates 5-methylcytosine in the sequence was considered (Figure 2E). The results revealed that 32% of the analyzed cytosines were methylated in Msh2 mutant mice compared to 11% in their Msh2 WT controls (Figure 2E). The 2.9-fold increase in the methylated cytosines of *DKK1* in Msh2 mutant CECs indicates that its reduced expression is dependent on DNA hypermethylation, mediated by loss of MMR function.

MMR deficiency is associated with abnormal differentiation of goblet cells

The marked increase in the stem cell signature (Figure 1B and C) and the reduced p21$^{CIP1/WAF1}$ expression in Msh2 mutant colonic crypts (Figure 1D) suggest that the normal cell differentiation may be disturbed. This prompted us to investigate the expression of known markers for specific differentiated cells in the colon. We measured a significant increase in the mRNA level of the goblet cell marker *Muc2* (Figure 3A) in Msh2 mutant CECs that was also confirmed in colonic tissue sections stained with Muc2-specific antibody (Figure 3B). In addition, the expression of Klf4, the main transcription factor that regulates the differentiation of intestinal goblet cells (Katz et al., 2002), was 1.8-fold reduced in Msh2$^{-/-}$ CECs (Figure 3A), leading us to further hypothesize that the normal development of the goblet cells might be impacted.

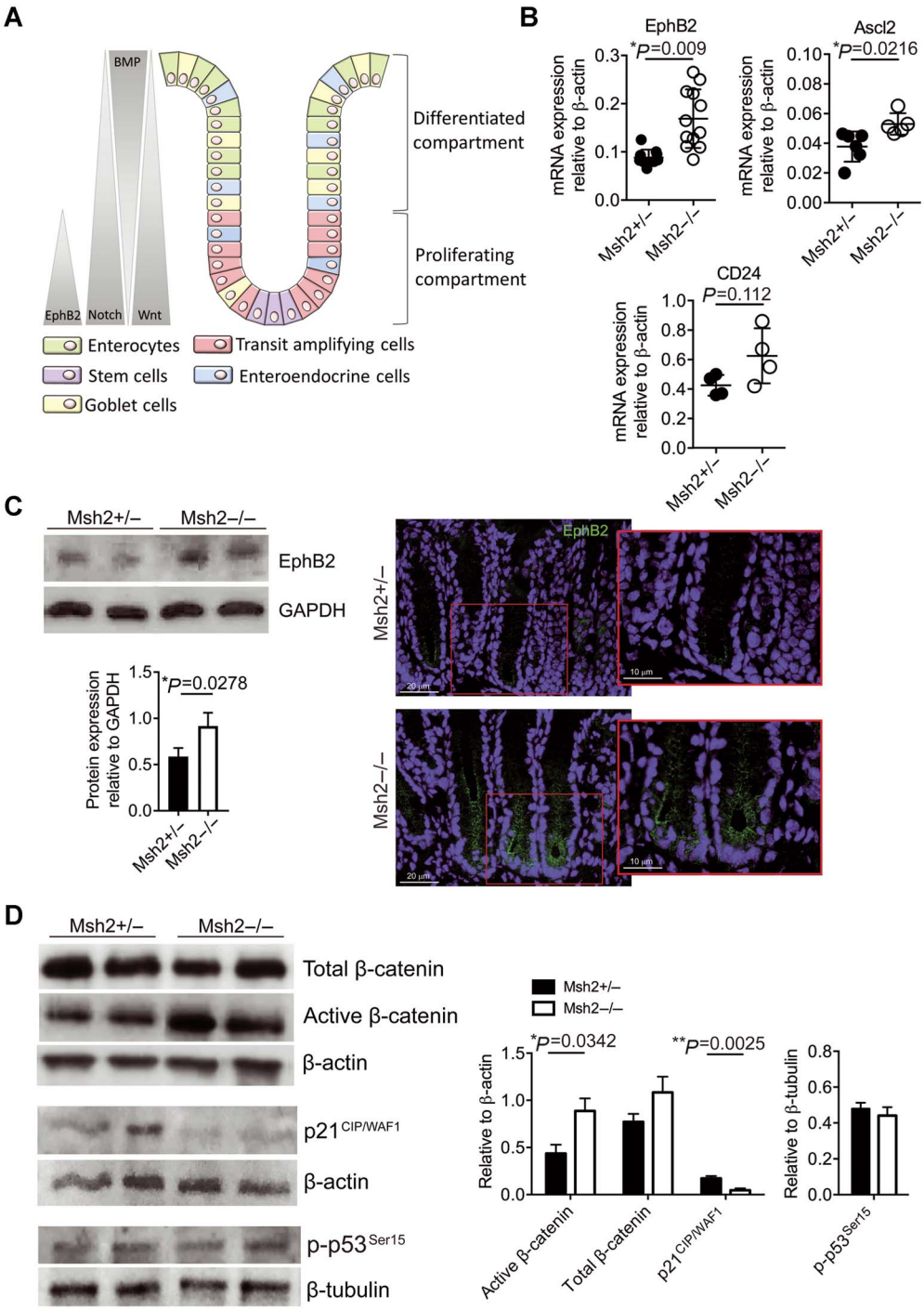

Figure 1 MMR deficiency mediates strong stem cell-like phenotype that supports enhanced proliferation in CECs. (**A**) A typical colonic crypt that comprises stem cells, progenitor cells (TA cells), and differentiated cells (goblet, enterocytes, and enteroendocrine cells). The gradient expression of WNT, Notch, and BMP pathways as well as EphB2 is denoted. (**B**) mRNA expression levels of the stem cell markers *EphB2*, *Ascl2*, and *CD24* relative to β-actin in $Msh2^{+/-}$ and $Msh2^{-/-}$ CECs. Each dot represents an individual mouse. (**C**) Western blot analysis of EphB2 expression in CECs from $Msh2^{+/-}$ and $Msh2^{-/-}$ mice and representative images showing its expression in $Msh2^{+/-}$ and $Msh2^{-/-}$ colonic crypts. The intensity of western blot bands relative to their respective GAPDH bands was measured by densitometry analysis and ImageJ. This analysis was carried out with three individual mice per genotype from three individual western blots. Scale bar, 20 μm (main) and 10 μm (enlarged). (**D**) Protein expression of active and total β-catenin, $p21^{CIP1/WAF1}$, and $p\text{-}p53^{Ser15}$ in $Msh2^{+/-}$ and $Msh2^{-/-}$ CECs. The intensity of western blot bands relative to their respective β-actin or β-tubulin bands was determined by densitometry analysis and ImageJ in three individual mice per genotype.

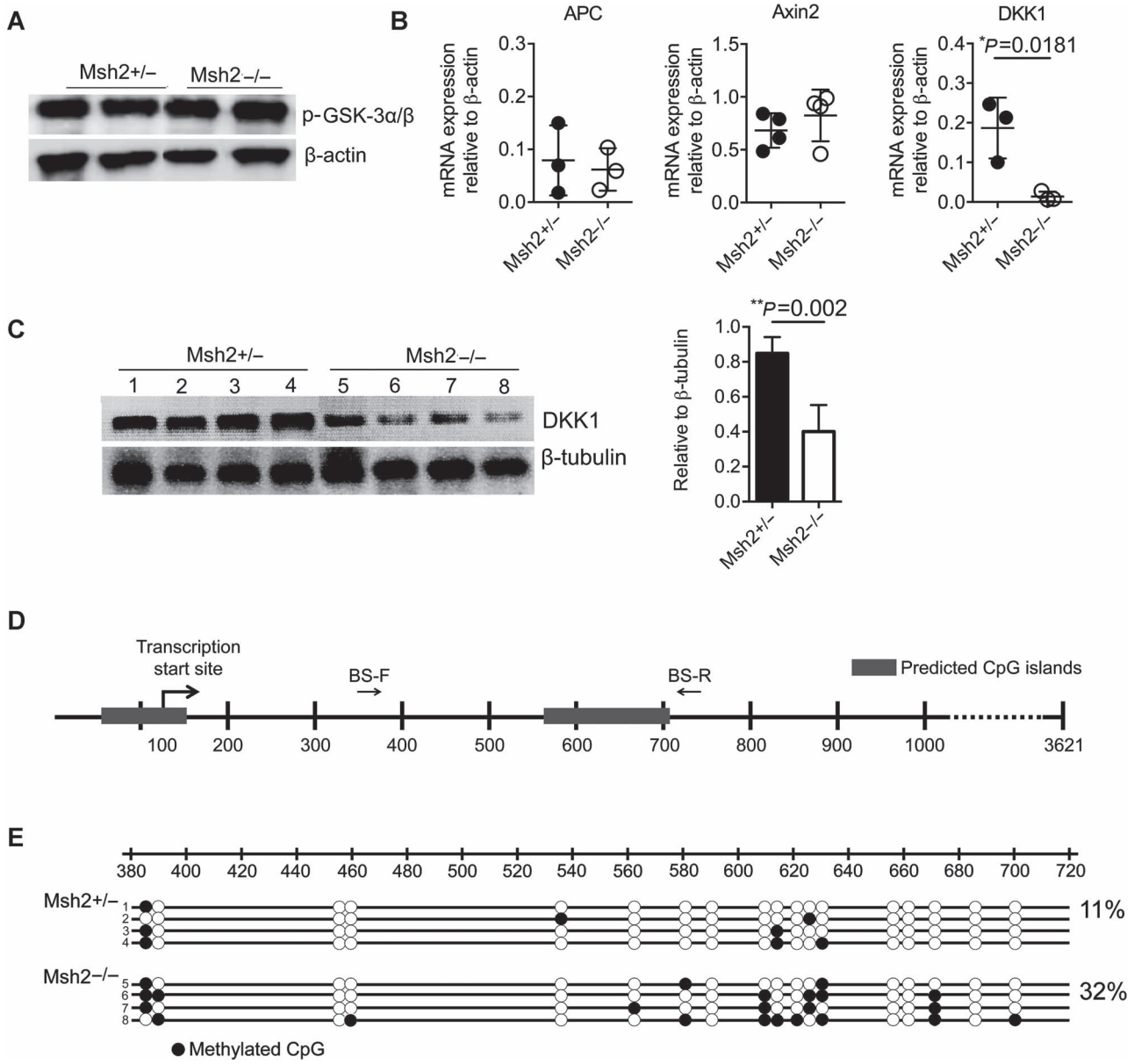

Figure 2 Analysis of the main factors involved in the regulation of WNT signaling. (**A**) Representative western blot of active p-GSK-3α/β (Tyr279/216) in Msh2$^{+/-}$ and Msh2$^{-/-}$ CECs. (**B**) mRNA expression levels of the components of the β-catenin destruction complex, *APC* and *Axin2*, and the WNT signaling pathway inhibitor *DKK1* in Msh2$^{+/-}$ and Msh2$^{-/-}$ CECs. (**C**) Expression of DKK1 in Msh2$^{+/-}$ and Msh2$^{-/-}$ CECs detected by western blot. The numbers indicate individual mice. The intensity of western blot bands relative to their respective β-tubulin bands was measured by densitometry analysis using ImageJ in three individual mice per genotype. (**D**) Schematic representation of the *DKK1* region containing two CpG islands. The position of the transcription start site, the CpG islands, and the primers used in the methylation-specific PCR are shown. (**E**) Bisulfite sequencing analysis of the *DKK1* CpG island (+380 to +720). Genomic DNA isolated from purified CECs, matching the cell lysates used for western blot in **C**, was used for bisulfite sequencing analysis. The numbers on the left correspond to the individual mice also used in **C**. Open circles indicate unmethylated cytosines, and black circles show methylated cytosines. Percentages indicate the fraction of methylated cytosines.

To investigate this possibility, we stained colonic tissue with periodic acid–Schiff (PAS), a specific dye that stains mucins and enables visualization of goblet cells (Figure 3C). In agreement with the above results, the PAS staining produced more intensive staining pattern in Msh2-deficient colonic tissue compared to their WT controls, indicating an increase in the mucin compounds. In addition, we counted less goblet cells per colonic crypt in Msh2$^{-/-}$ mice, which was more prominent in the distal part of the colon (Figure 3C) and correlated with the reduced expression levels of Klf4.

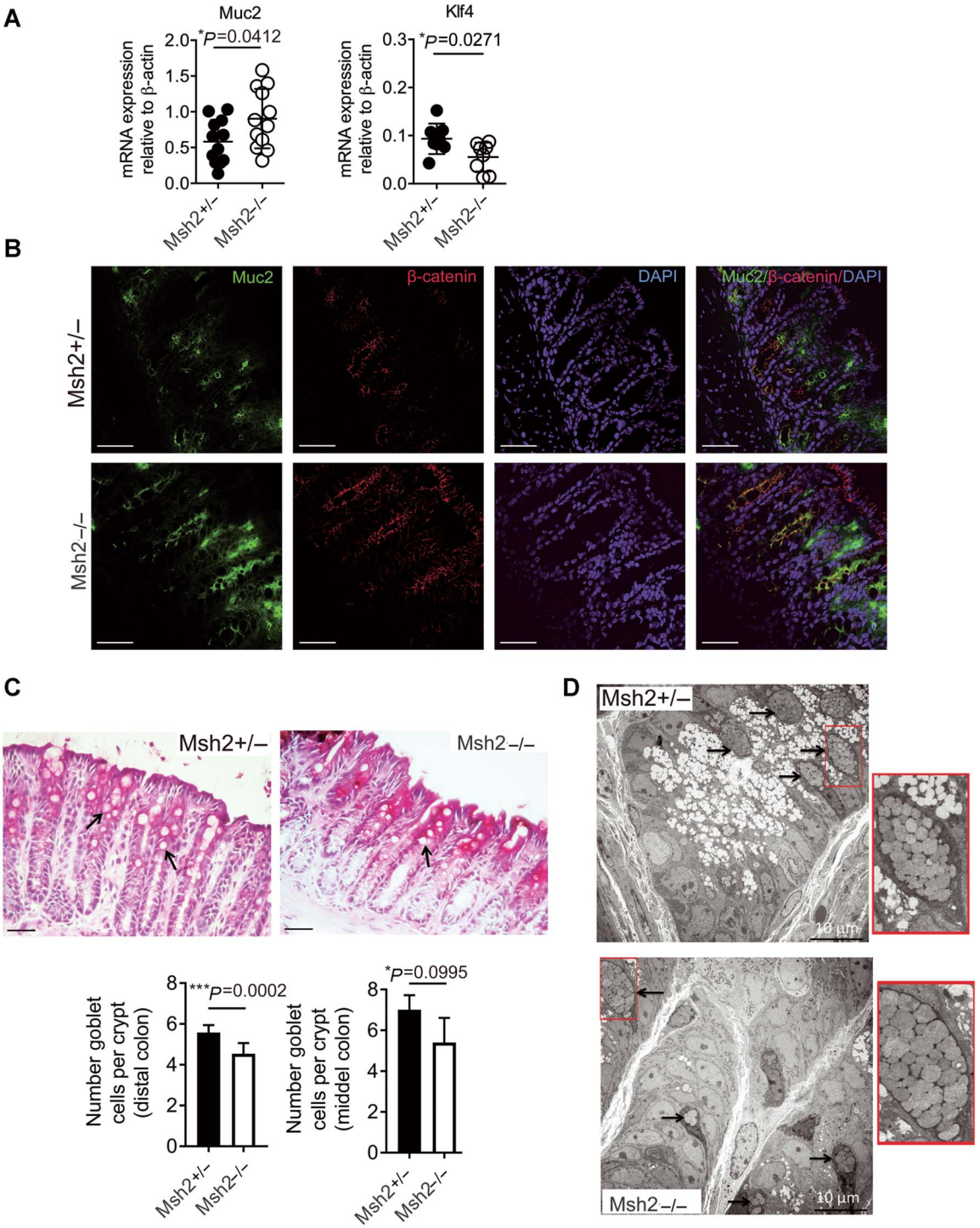

Figure 3 MMR deficiency impacts the normal differentiation and function of the intestinal goblet cells. (**A**) mRNA expression levels of the goblet cell-specific markers *Muc2* and *Klf4*. (**B**) Expression of Muc2 protein (green) and β-catenin (red) in Msh2$^{+/-}$ and Msh2$^{-/-}$ colonic crypts. Scale bar, 20 µm. (**C**) Goblet cells visualized by staining of colonic tissue with PAS reagent. Mucins that are produced by the goblet cells are stained in magenta. The number of goblet cells per colonic crypt is determined by averaging the number of goblet cells counted in at least seven morphologically well-preserved crypts of each mouse ($n = 6$). Scale bar, 20 µm. (**D**) Transmission electron microscopy (TEM) analysis of goblet cells (indicated by arrows) showing differences in their cell size and mucin-loaded vesicles. Scale bar, 10 µm.

Furthermore, we assessed the morphology of the goblet cells using electron microscopy. Our analysis revealed two important features. The first and most striking was the observation that in Msh2$^{-/-}$ mice the goblet cells had notably larger mucin-loaded vesicles compared to their WT controls (Figure 3D). Second, some of the goblet cells in Msh2$^{-/-}$ mice were smaller in size (Figure 3D), suggesting for lack of maturity of these cells.

To investigate the development of the colonic enterocytes, we measured the expression of their main product sucrase-isomaltase (*SIM*) and two transcription factors hepatocyte nuclear factor 1 beta (Hnf1β) and homeobox protein Cdx2 that regulate their terminal differentiation (Benoit et al., 2010; D'Angelo et al., 2010). The results showed no differences in the mRNA levels of these genes (Figure 4A). Other specific characteristics for mature enterocytes such as cell polarization and microvilli development were also not different between the genotypes (Figure 4B). Furthermore, the development of the colonic enteroendocrine cells was also unaffected by the loss of MMR function, as indicated by the expression levels of synaptophysin (*SYP*) and Nk2 homeobox 2 (Nkx2.2), the transcription factor shown to regulate their differentiation (Desai et al., 2008; Figure 4C). Taken together, the results indicate that inactivation of MMR system leads not only to changes in the proliferative but also in the differentiated cell compartment, specifically affecting the normal goblet cell development and function.

Regulation of the colonic homeostasis in Msh2$^{-/-}$ mice

Here we present evidence that in Msh2 mutant mice deregulated WNT signaling leads to an increased stem cell-like phenotype, enhanced proliferation, and abnormal goblet cell development and function. In general, the proliferation and differentiation in the colonic crypts are precisely regulated by the interplay between WNT, BMP, and Notch pathways. WNT signaling maintains proliferation, while the BMP pathway regulates the differentiation of the colonocytes (Medema and Vermeulen, 2011). Notch seems to have dual functions in the colonic crypt by being responsible for directing both proliferation and differentiation (VanDussen et al., 2012). Therefore, we assessed whether the Notch and BMP signaling pathways function normally in Msh2 mutant colonic epithelium. First, we examined the expression of the Notch-responsive gene *Hes1* that mediates reduction in the members of the secretory lineage (i.e. goblet and enteroendocrine cells) and expansion of the absorptive enterocytes (Stanger et al., 2005). However, *Hes1* expression was normal in Msh2-deficient CECs (Figure 5A). On the other hand, loss in the Notch activity will normally lead to an induction of *Math1* expression in the colonic crypts (van Es et al., 2005). Similarly, *Math1* mRNA levels were not affected by the Msh2 mutant genotype (Figure 5A), suggesting that Notch activity is not altered under Msh2-deficient background. Next, we investigated the expression of major BMP signaling components since downregulation of BMP signaling has been shown to impact the goblet cell terminal differentiation (Auclair et al., 2007). Our results showed a significant increase of *BMPR2* and *BMP2* mRNA levels in Msh2-deficient cells (Figure 5B). We also detected higher protein expression of BMP2 and BMP4 ligands in Msh2 mutant colonic crypts by immunofluorescence. BMP2 and BMP4 ligands were expressed predominantly by differentiated (Ki-67-negative) cells (Figure 5C), suggesting for elevated BMP activity in Msh2-deficient mice.

Taken together, our results demonstrate that MMR system plays a key role in the maintenance of the colonic homeostasis. Here we show that under MMR-deficient background increased methylation of *DKK1* causes elevated WNT/β-catenin activity that results is strong stem cell-like phenotype and increased proliferation. In addition to the elevated WNT, the BMP signaling was also increased. These events impact the normal goblet cell development and function and hence the colonic homeostasis.

Discussion

Inactivation of MMR pathway in CECs leads to abnormal proliferation compared to their WT controls, a feature that highly predisposes these cells to transformation (Belcheva et al., 2014). Although it has been suggested that this is caused by overactivation of WNT/β-catenin, the mechanistic details were not elucidated. In the present study, we investigated the causative factors that mediate deregulated WNT signaling in MMR-deficient CECs and its impact on the colonic homeostasis. We first tested whether the enhanced proliferation in Msh2 mutant CECs correlates with specific pattern of stem cell markers and found significant increase in mRNA expression levels of *EphB2*, *EphB3*, *CD44* (in agreement with our previous study) (Belcheva et al., 2014), and *Ascl2*. Another stem cell marker *CD24*, although not significant, was also elevated in Msh2 mutant cells (Figure 1B; Supplementary Figure S2). The change in the expression of *EphB2* and *EphB3* is particularly interesting. Eph receptors belong to a family of receptor tyrosine kinases and are highly abundant in proliferating cells and gradually decrease in differentiated cells (Figure 1A). The Eph receptors and their cognate ligands are important in defining the cell positioning and migration within the intestinal crypts (Guo et al., 2006). Because EphB proteins are directly regulated by β-catenin and are expressed by proliferating cells, they have been implicated in CRC development (Batlle et al., 2002; Jägle et al., 2014). However, the role of EphB proteins in the process of carcinogenesis seems to be very controversial. Reduction of EphB2 and EphB3 expression has been found in advanced stages of colon cancer where the extent of EphB2 expression correlates with the cancer aggressiveness (Batlle et al., 2005; Guo et al., 2006; Jägle et al., 2014). In contrast, Merlos-Suárez et al. (2011) have reported that EphB2 defines strong proliferating capacity of CECs and has distinct cancer initiating properties. In this study, we show evidence that EphB2 expression follows the typical gradient pattern, which however, is considerably prolonged in Msh2-deficient colonic crypts (Figure 1C). How the increased EphB2 expression in Msh2 mutant CECs is related to their enhanced proliferative potential and high cancer susceptibility still remains to be investigated.

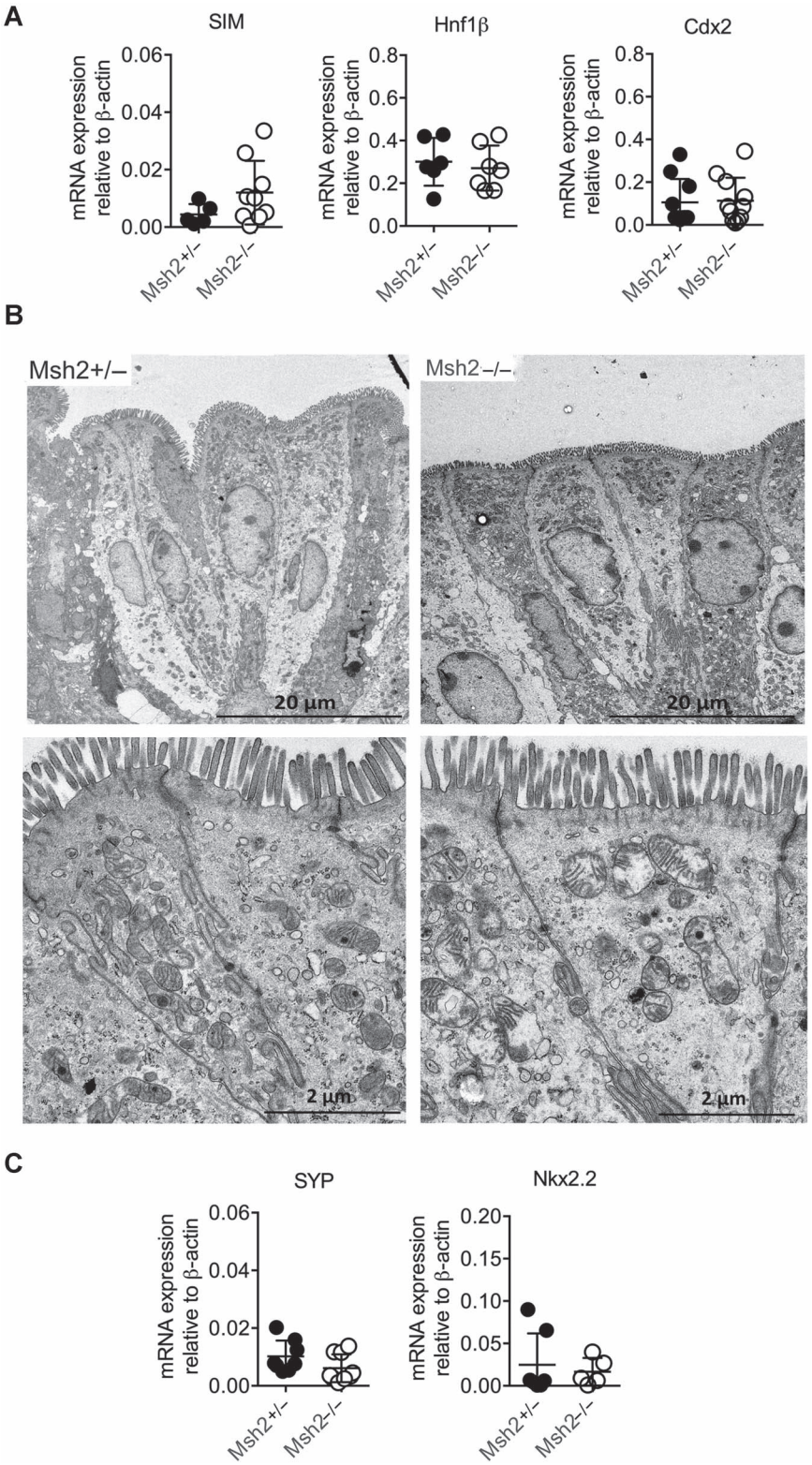

Figure 4 Analysis of the enterocytes and enteroendocrine cells in Msh2 mutant mice. (**A**) Analysis of the mRNA levels of *SIM*, a specific marker of intestinal enterocytes, and the transcription factors *Hnf1β* and *Cdx2* that regulate their differentiation. (**B**) Representative TEM pictures showing normal enterocyte morphology, cell polarity, and microvilli formation. Scale bar, 20 µm (upper) and 2 µm (lower). (**C**) Analysis of mRNA expression of *SYP* and *Nkx2.2* markers for intestinal enteroendocrine cells.

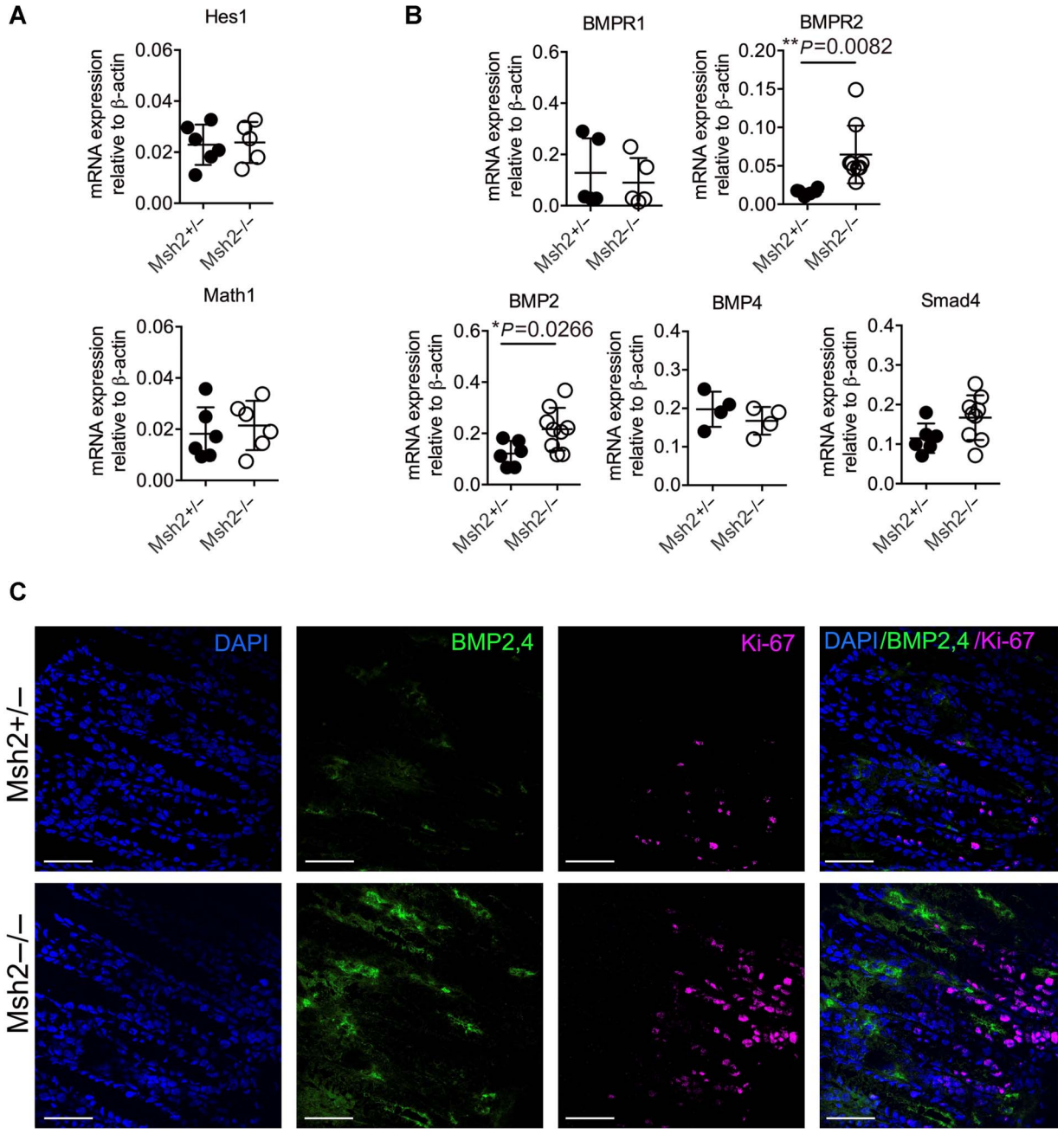

Figure 5 Analysis of Notch and BMP signaling pathways in colonic tissue derived from Msh2 mutant mice. (**A**) The expression levels of the Notch-responsive genes *Hes1* and *Math1* are shown relative to β-actin. (**B**) mRNA expression levels of BMP receptors *BMPR1* and *BMPR2*, BMP ligands *BMP2* and *BMP4*, and the signal transducer *Smad4*. (**C**) Expression of BMP2 and BMP4 ligands (BMP2,4; green) and the proliferation marker Ki-67 (magenta) in colonic crypts from $Msh2^{+/-}$ and $Msh2^{-/-}$ mice. Scale bar, 20 µm.

Furthermore, our results suggest that the enhanced stem cell-like phenotype and increased proliferation result from excessive levels of the active form of β-catenin (Figure 1D). In addition, this was concomitant with loss of expression of the negative cell cycle regulator $p21^{CIP1/WAF1}$ (Figure 1D). The expression of p21 can be induced by p53 (Gartel and Tyner, 1999) or negatively regulated by β-catenin (Kamei et al., 2003). Specifically, $p53^{Ser15}$ phosphorylation is required for transcriptional activation of the p21 promoter (Loughery et al., 2014). Therefore, we investigated whether the loss of p21 in Msh2 mutant CECs is caused by reduced $p53^{Ser15}$ levels in $Msh2^{-/-}$ cells (Figure 1D). The result showed that $p53^{Ser15}$ expression was similar between Msh2 mutant and Msh2 WT CECs, suggesting that loss of p21 is caused by p53-independent mechanism. It has been shown that overactivation of WNT leads to induction of c-Myc that represses p21 transcription to efficiently maintain proliferation and

suppress differentiation (van de Wetering et al., 2002). Therefore, the reduction of p21 in Msh2 mutant mice likely results from the overactive WNT and contributes to the increased proliferation capacity of the CECs.

To further understand the causative factors leading to the excessive levels of the active β-catenin in Msh2-deficient CECs, we investigated the activity of WNT pathway upstream of β-catenin. Since GSK-3β plays a key role in the phosphorylation of β-catenin in response to environmental signals (van de Wetering et al., 2002), it was important to investigate changes in its activity between the genotypes. We found that the active form of the kinase (p-GSK-3β^{Tyr216}) was not different between Msh2 mutant and Msh2 WT CECs (Figure 2A). We also investigated the expression of *APC* and *Axin2*, two key components of the β-catenin destruction complex that are also frequently mutated in MMR-deficient cells (Castiglia et al., 2008). However, we found that their expression was not altered in Msh2-deficient CECs (Figure 2B). These results, therefore, suggest that the excessive levels of active β-catenin in Msh2 mutant CECs result neither from discrete external stimuli that modulate the activity of GSK-3β, nor by loss of expression of *APC* or *Axin2*. Instead, we detected that both the mRNA and protein expression levels of the negative WNT regulator *DKK1* were dramatically lost in Msh2 mutant cells (Figure 2B and C). DKK1 is a secreted antagonist of WNT signaling. It has been suggested that the protein forms a ternary complex with LRP5/6 and Kremen receptors and mediates the endocytosis of this complex resulting in depletion of LRP5/6 from the cell surface (Niida et al., 2004). Indeed, DKK1 expression is also regulated by β-catenin/TCF and has been shown to function as an important negative feedback loop in WNT pathway. In this way, DKK1 plays a critical role in the precise control of the transmission of WNT signals and avoids abnormal signaling output. It is not surprising that DKK1 expression is often reduced in CRC (Gonzlez-Sancho et al., 2005). Since inactivation of the MMR system leads to 11-fold increase in the mutation frequency in intestinal epithelium (Andrew et al., 1997), we hypothesized that mutational inactivation of the *DKK1* gene may be the causative reason for the loss of DKK1 expression. However, no mutations were present in the *DKK1* sequences from Msh2 mutant CECs. Another mechanism that can lead to loss of *DKK1* is via hypermethylation of CpG regions (Aguilera et al., 2006; Sato et al., 2007). Since this process has been previously associated with inactivation of MMR (Rawson et al., 2011), we investigated the methylation status of *DKK1*. The gene has two regions containing high frequency of CpG sites that are potential targets for methylation. To assess the methylation status of the gene, we used methylation-specific PCR sequencing (Li and Tollefsbol, 2011); however, we were able to analyze only the CpG island located ∼600 bp downstream of the transcription start site (Figure 2D and E). The data revealed 2.9-fold increase in methylated cytosines in Msh2$^{-/-}$ CECs and indicated that loss of *DKK1* expression is likely caused by enhanced methylation of CpG regions in Msh2$^{-/-}$ CECs. Taken together, our results suggest that in Msh2 mutant CECs loss of DKK1 expression causes deregulation of WNT signaling resulting in excessive levels of active β-catenin that promotes strong stem cell-like properties and enhanced proliferation.

The abnormally high expression of stem cell markers, the prolonged gradient of EphB2, and the loss of p21$^{CIP1/WAF1}$ suggest that in Msh2 mutant colonic crypts the normal balance between proliferating and differentiated cells is disturbed. This prompted us to investigate the expression of several markers specific to the three types of differentiated cells in the colon: goblet, enterocytes, and enteroendocrine cells. We found that the goblet cell marker Muc2 was elevated at both mRNA and protein levels in Msh2 mutant CECs (Figure 3A and B). Muc2 is an important component of the intestinal barrier, and its expression is frequently reduced in CRC tumors compared to adjusted normal tissue. Also, loss of Muc2 expression correlates with poor prognosis in CRC (Kang et al., 2011; Wang et al., 2017). However, a small fraction of CRCs (10%–20%), known as mucinous colorectal adenocarcinomas, heavily express Muc2 (Perez et al., 2008). It has been suggested that the expression differences could arise from hypermethylation (Hanski et al., 1997) or hypomethylation (Gratchev et al., 2001) of the *Muc2* promoter. Several studies demonstrate that the regulation of *Muc2* is quite more complex and responds to different stimuli. The promoter region of the *Muc2* contains binding sites for p53 (Ookawa et al., 2002), AP1 elements, and consensus binding site for c-Myc (Velcich et al., 1997), suggesting that Muc2 overexpression could be associated by the enhanced WNT/β-catenin signaling. However, Muc2 overexpression can be induced also via activation of BMP pathway (Prakash et al., 2011). Because Muc2 is exclusively secreted by the intestinal goblet cells, we hypothesized that the increased expression of the protein in Msh2-deficient mice will correlate with an increase in the goblet cell numbers. To our surprise, we observed reduction in the goblet cells per colonic crypt (Figure 3C) that, however, contained larger mucin-loaded vesicles (Figure 3D). Also, we found that some of the goblet cells in Msh2-deficient mice were smaller in size compared to their WT controls (Figure 3D), suggesting for a delay in their maturation. We also investigated the expression of Klf4, a goblet cell differentiation marker, with key role in regulation of the proliferation/differentiation in the gut epithelium (Katz et al., 2002; Yu et al., 2016). The protein is almost undetectable in exponentially proliferating cells due to the suppressive action of β-catenin/TCF signaling (Shields et al., 1996; Flandez et al., 2008; Zhang et al., 2012), and its overexpression in colon cancer cells was shown to cause G1/S arrest (Chen et al., 2001). Deletion of Klf4 in mice abrogated specifically the differentiation of the intestinal goblet cells and was associated with increased WNT/β-catenin signaling and proliferation (Ghaleb et al., 2011). These studies demonstrate that Klf4 is a critical factor that directs the differentiation of the intestinal goblet cells. We found that Klf4 was downregulated by 1.8-fold in Msh2 mutant cells (Figure 3A). This result, therefore, correlates with the reduced goblet cell number and their delayed maturation (Figure 3C and D). The reduced Klf4 can also lead to an increase in the Muc2 production, as previously reported (Yu et al., 2016).

Interestingly, the other specialized cell types, namely enterocytes and enteroendocrine cells, were not altered under MMR-deficient background (Figure 4).

Taken together, these results indicate that inactivation of the MMR system leads to dramatic alterations in the stem cell and differentiated cell compartments and hence, disturbed colonic homeostasis.

The differentiation of the intestinal proliferating cells is regulated by the complex interplay between WNT, Notch, and BMP pathways. Specifically, activation of Notch signaling leads to induction of one of its responsive genes *Hes1* that further mediates reduction in the members of the secretory lineage and expansion of the absorptive cells (Stanger et al., 2005). On the other hand, loss in the Notch activity will lead to *Math1* expression in the colonic crypts (van Es et al., 2005). However, the expression of both genes (*Hes1* and *Math1*) was not altered between Msh2-deficient and Msh2 WT CECs, suggesting that Notch functions normally under Msh2-deficient background (Figure 5A). In addition, BMP pathway controls the terminal differentiation of the secretory cells. Since we observed alterations in the goblet cell differentiation and function, it was important to investigate the BMP signaling components and we measured an increase in *BMPR2* and *BMP2* mRNA levels in Msh2-deficient CECs (Figure 5B). Inactivation of BMP signaling in *Bmpr1a* mutant mice led to no differences in the number of goblet cells and *Muc2* expression, although they were smaller in size and contained smaller mucin granules (Auclair et al., 2007). Our results, therefore, suggest for unique changes in the goblet cell function that likely result from alterations in both WNT and BMP signaling. These results are intriguing, especially in the context of the cancer susceptibility of MMR-deficient CECs. While the tumor-promoting properties of WNT signaling are well documented, the role of BMP in carcinogenesis is very controversial. Because BMP is a natural antagonist of WNT, it was suggested that the pathway acts as a tumor suppressor (Hardwick et al., 2008). Yet, it has been shown that BMP4 overexpression promotes invasiveness of colon cancer cells (Deng et al., 2007), while BMP2 induces epithelial–mesenchymal transition, and hence, strengthening the metastatic potential of colon cancer cells (Kang et al., 2009; Kim et al., 2015). It was also shown that BMP pathway promotes growth of primary colon tumors *in vivo* (Lorente-Trigos et al., 2010). On the basis of this and other studies, the current hypothesis is that BMP initially may act as tumor suppressor and later as a tumor promoter. What are the specific conditions and factors that affect the biological effects of BMP pathway is poorly understood. Our results indicate that in Msh2-deficient CECs overactivation of WNT is concomitant with enhanced BMP activity. The physiological meaning of this crosstalk likely plays a central role in maintenance of the colonic homeostasis. Our work showed that in Msh2 mutant colonic crypts improper regulation of β-catenin activity promotes a crypt progenitor-like phenotype and increased proliferation that impact the normal differentiation and function of the goblet cells. To what extent the impaired homeostasis in MMR-deficient CECs is important in their susceptibility to transformation remains to be investigated.

Materials and methods

Mice

The $Msh2^{-/-}$ mice have been previously described (Reitmair et al., 1995). Briefly, 68 base pairs in the *Msh2* gene were deleted by neomycin resistance cassette that was inserted in an antisense orientation in exon 11. This has resulted in a loss of both copies of the *Msh2* allele ($Msh2^{-/-}$) and complete loss of Msh2 protein expression. All mice were on the C57BL/6J background and raised under specific pathogen-free conditions. *Msh2* heterozygous ($Msh2^{+/-}$) mice characterized by normal DNA repair were used as controls in this study. The mice were genotyped as previously described (Peters et al., 2003). All experiments and analysis were conducted with 6-week-old mice.

Isolation of CECs

Mouse colons were removed, flushed with PBS, cut into 0.5 cm pieces, and transferred in Ca^{2+}/Mg^{2+}-free PBS supplemented with 5 mM EDTA. The tissue was incubated for 20 min at 37°C. The solution was replaced with pure PBS, and CECs were released by vigorous shacking. Cells were collected by centrifugation at 1300 rpm for 5 min at 4°C. The procedure was repeated three times. The CECs were collected and used for mRNA or DNA isolation or cell lysates.

mRNA isolation and quantitative PCR

CECs were homogenized prior to RNA isolation using PureLink™ RNA Mini Kit (Ambion, Life Technologies) and reverse transcribed to cDNA using Maxima H Minus First Strand cDNA Synthesis Kit (Thermo Fischer Scientific). Relative quantification of gene expression was performed using PowerUp™ SYBR Green Master Mix (Applied Biosystems). QPCR was carried out with initial denaturation at 95°C for 10 min followed by 40 cycles of denaturation at 95°C for 15 sec and extension at 60°C for 1 min. Relative gene expression levels were calculated by ΔΔCt method and normalized to the reference gene β-actin. The primer sequences are shown in Supplementary Table S1.

Immunofluorescence

Frozen Swiss-rolled colons were cut into 5-µm-thick sections and fixed with ice-cold acetone. The tissue was blocked with 3% BSA in PBST for 1 h at room temperature and incubated with specific antibodies detecting Ki67 (Abcam), EphB2 (Cell Signaling Technology), Mucin 2 (F-2), BMP-2/4 (H-1), and total β-catenin (H-102) obtained from Santa Cruz Biotechnology. Typically, the primary antibodies were used at 1:100 dilution at 4°C for overnight incubation. Subsequently, tissue sections were washed three times with PBST and incubated with secondary antibodies goat anti-rabbit IgG Alexa-488 or Alexa-647 (Abcam) and goat anti-mouse IgG Alexa-488 (Santa Cruz Biotechnology) in 1:250 for 1 h at room temperature. Nuclei were counterstained with 4′,6-diamino-2-phenylindole (DAPI) obtained from

Sigma. The tissue was then covered with Fluoromount™ Aqueous Mounting Medium (Sigma) and imaging was performed with a Zeiss LSM510 confocal microscope at the Danish Molecular Biomedical Imaging Center (DaMBIC), University of Southern Denmark.

PAS staining

The 5-µm-thick sections were fixed with 10% formalin followed by hydration in water. The tissue was stained with periodic acid solution (Sigma) for 5 min, Schiff's reagent for 15 min, and hematoxylin solution for 90 sec. Samples were dehydrated in increasing concentrations of ethanol (70%, 90%, 95%, and 100%) followed by incubation in xylene and finally sealed with a coverslip using Fisher Chemical™ Permount™ Mounting Medium (Fisher Scientific). Goblet cells were observed and counted in individual well-preserved colonic crypts using a Leica DMRBE microscope.

TEM

A fragment of the distal part of the mouse colon was obtained and the tissue was fixed and processed for TEM imaging according to standard methods (Almeida Junior et al., 2017). Goblet cells and enterocytes were observed using a JEOL 1400 plus transmission electron microscope at the Department of Pathology, Odense University Hospital.

Western blotting

Isolated CECs were lysed with RIPA buffer (150 mM sodium chloride, 1% Triton X-100, 0.1% SDS, 50 mM Tris, pH 8.0) containing protease inhibitor cocktail (Sigma). The proteins were separated by 10%–15% SDS–PAGE and blotted onto a PVDF membrane (Bio-Rad). Membranes were blocked in TBS containing 0.1% Tween® 20 (Fisher BioReagents) and 5% skim milk powder (Oxoid) for 1 h at room temperature. Membranes were incubated with total β-catenin (H-102) (Santa Cruz Biotechnology), non-phospho (active) β-catenin (Ser33/37/Thr41), p-53 (Ser15) and EphB2 (D2X2I) obtained from Cell Signaling, or p-GSK-3α/β (Tyr279/216), p21 (F-5), and DKK-1 (B-7) from Santa Cruz Biotechnology. β-actin (Cell Signaling), GAPDH (Sigma), or β-tubulin (Thermo Fisher Scientific) was used as loading control. Typically, the primary antibodies were used at 1:1000 at 4°C overnight incubation. After washing three times with TBST, the membranes were incubated with goat anti-rabbit IgG-AP (Santa Cruz Biotechnology) or goat anti-mouse IgG-AP (Cell Signaling) at 1:20000 for 1 h at room temperature. Protein–antibody complexes were visualized using a chemiluminescent substrate Tropix® CDP-*Star*® (Applied Biosystems) and detected on CL-X Posure™ Film (Thermo Scientific). Each western blot was repeated at least three times, and the protein expression levels were determined by densitometry analysis and ImageJ.

DKK1 gene sequencing and CpG island methylation analysis

Genomic DNA from CECs derived from four $Msh2^{+/-}$ and four $Msh2^{-/-}$ mice was isolated using the GenElute™ Mammalian Genomic DNA Miniprep Kit (Sigma). The *DKK1* gene was amplified using primer sequences listed in Supplementary Table S2 and the Phusion High-Fidelity PCR Kit (Thermo Fisher Scientific). PCR conditions consisted of initial denaturation at 98°C for 3 min followed by 35 cycles of denaturation at 98°C for 10 sec, annealing at 63°C for 30 sec, and extension at 72°C for 2 min completed with final extension at 72°C for 10 min. The PCR products were analyzed on 1% agarose gel and bands corresponding to 3570 bp PCR product were cut out, and DNA was purified using the GeneJET Gel Extraction Kit (Thermo Fisher Scientific).

For analyses of the methylation status of *DKK1*, genomic DNA was bisulfite converted using the EpiTect® Bisulfite Kit (Qiagen). A region encompassing a predicted CpG island was amplified with specific primers for bisulfite conversion-based PCR. The primers were designed using MethPrimer Version 2.0 (primer sequences are listed in Supplementary Table S2). The JumpStart™ Taq DNA Polymerase (Sigma) was applied, and PCR conditions consisted of initial denaturation at 94°C for 3 min followed by 40 cycles of denaturation at 94°C for 30 sec, annealing at 59°C for 30 sec, and extension at 72°C for 1 min completed with final extension at 72°C for 10 min. PCR products were analyzed by 1.5% agarose gel electrophoresis, and bands corresponding to 388 bp were gel extracted and submitted to sequencing. All samples, i.e. the entire *DKK1* gene and the methylation-specific PCR-purified products, were sequenced by Eurofins Genomics using the same primers as used for PCR amplifications. Bisulfite sequencing DNA methylation data were analyzed with the BDPC DNA methylation analysis platform (BISMA).

Statistical analysis

Data are presented as mean ± standard deviation. All graphically presented data were analyzed using GraphPad Prism version 7.0 and two-tailed *t*-tests. A value of $P < 0.05$ was considered statistically significant. Asterisks are defined as $*P < 0.05$, $**P < 0.01$, and $***P < 0.001$.

Acknowledgements

The authors acknowledge the Danish Molecular Biomedical Imaging Center (DaMBIC, University of Southern Denmark) for use of the bioimaging facilities, as well as Henrik Schrøder (Department of Pathology, Odense University Hospital) for use of the electron microscope. We also thank Barbara Guerra for helpful discussions and technical help.

Funding

This project is funded by the Department of Biochemistry and Molecular Biology at University of Southern Denmark.

Conflict of interest: none declared.

Author contributions: K.N. and A.B. designed the study. K.N. planned the experiments, conducted data collection and analysis, and wrote the manuscript. C.M., N.C., M.L.C., C.L.M., and S.S.N. contributed to data collection and preparation of the manuscript. T.E.T. provided important reagents and helped with

analysis of the results and preparation of the manuscript. A.B. designed and supervised the study, performed data collection and analysis, and wrote the manuscript.

References

Aguilera, O., Fraga, M.F., Ballestar, E., et al. (2006). Epigenetic inactivation of the Wnt antagonist DICKKOPF-1 (DKK-1) gene in human colorectal cancer. Oncogene *25*, 4116–4121.

Almeida Junior, L.D., Quaglio, A.E.V., de Almeida Costa, C.A.R., et al. (2017). Intestinal anti-inflammatory activity of ground cherry (Physalis angulata L.) standardized CO_2 phytopharmaceutical preparation. World J. Gastroenterol. *23*, 4369–4380.

Andrew, S.E., Reitmair, A.H., Fox, J., et al. (1997). Base transitions dominate the mutational spectrum of a transgenic reporter gene in MSH2 deficient mice. Oncogene *15*, 123–129.

Artavanis-Tsakonas, S., Rand, M.D., and Lake, R.J. (1999). Notch signaling: cell fate control and signal integration in development. Science *284*, 770–776.

Auclair, B.A., Benoit, Y.D., Rivard, N., et al. (2007). Bone morphogenetic protein signaling is essential for terminal differentiation of the intestinal secretory cell lineage. Gastroenterology *133*, 887–896.

Batlle, E., Bacani, J., Begthel, H., et al. (2005). EphB receptor activity suppresses colorectal cancer progression. Nature *435*, 1126–1130.

Batlle, E., Henderson, J.T., Beghtel, H., et al. (2002). β-catenin and TCF mediate cell positioning in the intestinal epithelium by controlling the expression of EphB/ephrinB. Cell *111*, 251–263.

Belcheva, A., Irrazabal, T., Robertson, S.J., et al. (2014). Gut microbial metabolism drives transformation of MSH2-deficient colon epithelial cells. Cell *158*, 288–299.

Benoit, Y.D., Paré, F., Francoeur, C., et al. (2010). Cooperation between HNF-1α, Cdx2, and GATA-4 in initiating an enterocytic differentiation program in a normal human intestinal epithelial progenitor cell line. Am. J. Physiol. Gastrointest. Liver Physiol. *298*, G504–G517.

Boland, C.R., and Goel, A. (2010). Microsatellite instability in colorectal cancer. Gastroenterology *138*, 2073–2087.e3.

Castiglia, D., Bernardini, S., Alvino, E., et al. (2008). Concomitant activation of Wnt pathway and loss of mismatch repair function in human melanoma. Genes Chromosomes Cancer *47*, 614–624.

Chao, E.C., and Lipkin, S.M. (2006). Molecular models for the tissue specificity of DNA mismatch repair-deficient carcinogenesis. Nucleic Acids Res. *34*, 840–852.

Chen, X., Johns, D.C., Geiman, D.E., et al. (2001). Krüppel-like factor 4 (gut-enriched Krüppel-like factor) inhibits cell proliferation by blocking G1/S progression of the cell cycle. J. Biol. Chem. *276*, 30423–30428.

D'Angelo, A., Bluteau, O., Garcia-Gonzalez, M.A., et al. (2010). Hepatocyte nuclear factor 1α and β control terminal differentiation and cell fate commitment in the gut epithelium. Development *137*, 1573–1582.

Deng, H., Ravikumar, T.S., and Yang, W.L. (2007). Bone morphogenetic protein-4 inhibits heat-induced apoptosis by modulating MAPK pathways in human colon cancer HCT116 cells. Cancer Lett. *256*, 207–217.

Desai, S., Loomis, Z., Pugh-Bernard, A., et al. (2008). Nkx2.2 regulates cell fate choice in the enteroendocrine cell lineages of the intestine. Dev. Biol. *313*, 58–66.

Flandez, M., Guilmeau, S., Blache, P., et al. (2008). KLF4 regulation in intestinal epithelial cell maturation. Exp. Cell Res. *314*, 3712–3723.

Gartel, A.L., and Tyner, A.L. (1999). Transcriptional regulation of the $p21^{WAF1/CIP1}$ gene. Exp. Cell Res. *246*, 280–289.

Ghaleb, A.M., McConnell, B.B., Kaestner, K.H., et al. (2011). Altered intestinal epithelial homeostasis in mice with intestine-specific deletion of the Krüppel-like factor 4 gene. Dev. Biol. *349*, 310–320.

González-Sancho, J.M., Aguilera, O., García, J.M., et al. (2005). The Wnt antagonist DICKKOPF-1 gene is a downstream target of β-catenin/TCF and is downregulated in human colon cancer. Oncogene *24*, 1098–1103.

Gratchev, A., Siedow, A., Bumke-Vogt, C., et al. (2001). Regulation of the intestinal mucin MUC2 gene expression in vivo: evidence for the role of promoter methylation. Cancer Lett. *168*, 71–80.

Guo, D.L., Zhang, J., Yuen, S.T., et al. (2006). Reduced expression of EphB2 that parallels invasion and metastasis in colorectal tumours. Carcinogenesis *27*, 454–464.

Hanski, C., Riede, E., Gratchev, A., et al. (1997). MUC2 gene suppression in human colorectal carcinomas and their metastases: in vitro evidence of the modulatory role of DNA methylation. Lab. Invest. *77*, 685–695.

Hardwick, J.C., Kodach, L.L., Offerhaus, G.J., et al. (2008). Bone morphogenetic protein signalling in colorectal cancer. Nat. Rev. Cancer *8*, 806–812.

Heyer, J., Yang, K., Lipkin, M., et al. (1999). Mouse models for colorectal cancer. Oncogene *18*, 5325–5333.

Ionov, Y., Peinado, M.A., Malkhosyan, S., et al. (1993). Ubiquitous somatic mutations in simple repeated sequences reveal a new mechanism for colonic carcinogenesis. Nature *363*, 558–561.

Jägle, S., Rönsch, K., Timme, S., et al. (2014). Silencing of the EPHB3 tumor-suppressor gene in human colorectal cancer through decommissioning of a transcriptional enhancer. Proc. Natl Acad. Sci. USA *111*, 4886–4891.

Jensen, J., Pedersen, E.E., Galante, P., et al. (2000). Control of endodermal endocrine development by Hes-1. Nat. Genet. *24*, 36–44.

Jiricny, J. (2006). The multifaceted mismatch-repair system. Nat. Rev. Mol. Cell Biol. *7*, 335–346.

Kamei, J., Toyofuku, T., and Hori, M. (2003). Negative regulation of p21 by β-catenin/TCF signaling: a novel mechanism by which cell adhesion molecules regulate cell proliferation. Biochem. Biophys. Res. Commun. *312*, 380–387.

Kang, H., Min, B.S., Lee, K.Y., et al. (2011). Loss of E-cadherin and MUC2 expressions correlated with poor survival in patients with stages II and III colorectal carcinoma. Ann. Surg. Oncol. *18*, 711–719.

Kang, M.H., Kang, H.N., Kim, J.L., et al. (2009). Inhibition of PI3 kinase/Akt pathway is required for BMP2-induced EMT and invasion. Oncol. Rep. *22*, 525–534.

Katz, J.P., Perreault, N., Goldstein, B.G., et al. (2002). The zinc-finger transcription factor Klf4 is required for terminal differentiation of goblet cells in the colon. Development *129*, 2619–2628.

Kim, B.R., Oh, S.C., Lee, D.H., et al. (2015). BMP-2 induces motility and invasiveness by promoting colon cancer stemness through STAT3 activation. Tumour Biol. *36*, 9475–9486.

Lee, K., Tosti, E., and Edelmann, W. (2016). Mouse models of DNA mismatch repair in cancer research. DNA Repair *38*, 140–146.

Li, Y., and Tollefsbol, T.O. (2011). DNA methylation detection: bisulfite genomic sequencing analysis. Methods Mol. Biol. *791*, 11–21.

Li, Z., Pearlman, A.H., and Hsieh, P. (2016). DNA mismatch repair and the DNA damage response. DNA Repair *38*, 94–101.

Lorente-Trigos, A., Varnat, F., Melotti, A., et al. (2010). BMP signaling promotes the growth of primary human colon carcinomas in vivo. J. Mol. Cell Biol. *2*, 318–332.

Loughery, J., Cox, M., Smith, L.M., et al. (2014). Critical role for p53-serine 15 phosphorylation in stimulating transactivation at p53-responsive promoters. Nucleic Acids Res. *42*, 7666–7680.

Marra, G., and Jiricny, J. (2005). DNA mismatch repair and colon cancer. Adv. Exp. Med. Biol. *570*, 85–123.

Medema, J.P., and Vermeulen, L. (2011). Microenvironmental regulation of stem cells in intestinal homeostasis and cancer. Nature *474*, 318–326.

Merlos-Suárez, A., Barriga, F.M., Jung, P., et al. (2011). The intestinal stem cell signature identifies colorectal cancer stem cells and predicts disease relapse. Cell Stem Cell *8*, 511–524.

Modrich, P., and Lahue, R. (1996). Mismatch repair in replication fidelity, genetic recombination, and cancer biology. Annu. Rev. Biochem. *65*, 101–133.

Negureanu, L., and Salsbury, F.R., Jr. (2012). The molecular origin of the MMR-dependent apoptosis pathway from dynamics analysis of MutSα-DNA complexes. J. Biomol. Struct. Dyn. *30*, 347–361.

Niida, A., Hiroko, T., Kasai, M., et al. (2004). DKK1, a negative regulator of Wnt signaling, is a target of the β-catenin/TCF pathway. Oncogene *23*, 8520–8526.

Ookawa, K., Kudo, T., Aizawa, S., et al. (2002). Transcriptional activation of the MUC2 gene by p53. J. Biol. Chem. *277*, 48270–48275.

Pattyn, F., Hoebeeck, J., Robbrecht, P., et al. (2006). methBLAST and methPrimerDB: web-tools for PCR based methylation analysis. BMC Bioinformatics *7*, 496.

Perez, R.O., Bresciani, B.H., Bresciani, C., et al. (2008). Mucinous colorectal adenocarcinoma: influence of mucin expression (Muc1, 2 and 5) on clinicopathological features and prognosis. Int. J. Colorectal Dis. *23*, 757–765.

Peters, A.C., Young, L.C., Maeda, T., et al. (2003). Mammalian DNA mismatch repair protects cells from UVB-induced DNA damage by facilitating apoptosis and p53 activation. DNA Repair *2*, 427–435.

Pinto, D., Gregorieff, A., Begthel, H., et al. (2003). Canonical Wnt signals are essential for homeostasis of the intestinal epithelium. Genes Dev. *17*, 1709–1713.

Poulogiannis, G., Frayling, I.M., and Arends, M.J. (2010). DNA mismatch repair deficiency in sporadic colorectal cancer and Lynch syndrome. Histopathology *56*, 167–179.

Prakash, R., Bharathi Raja, S., Devaraj, H., et al. (2011). Up-regulation of MUC2 and IL-1β expression in human colonic epithelial cells by Shigella and its interaction with mucins. PLoS One *6*, e27046.

Rawson, J.B., Manno, M., Mrkonjic, M., et al. (2011). Promoter methylation of Wnt antagonists DKK1 and SFRP1 is associated with opposing tumor subtypes in two large populations of colorectal cancer patients. Carcinogenesis *32*, 741–747.

Reitmair, A.H., Schmits, R., Ewel, A., et al. (1995). MSH2 deficient mice are viable and susceptible to lymphoid tumours. Nat. Genet. *11*, 64–70.

Sato, H., Suzuki, H., Toyota, M., et al. (2007). Frequent epigenetic inactivation of DICKKOPF family genes in human gastrointestinal tumors. Carcinogenesis *28*, 2459–2466.

Schroder, N., and Gossler, A. (2002). Expression of Notch pathway components in fetal and adult mouse small intestine. Gene Expr. Patterns *2*, 247–250.

Schuijers, J., Junker, J.P., Mokry, M., et al. (2015). Ascl2 acts as an R-spondin/Wnt-responsive switch to control stemness in intestinal crypts. Cell Stem Cell *16*, 158–170.

Shields, J.M., Christy, R.J., and Yang, V.W. (1996). Identification and characterization of a gene encoding a gut-enriched Krüppel-like factor expressed during growth arrest. J. Biol. Chem. *271*, 20009–20017.

Stanger, B.Z., Datar, R., Murtaugh, L.C., et al. (2005). Direct regulation of intestinal fate by Notch. Proc. Natl Acad. Sci. USA *102*, 12443–12448.

van de Wetering, M., Sancho, E., Verweij, C., et al. (2002). The β-catenin/TCF-4 complex imposes a crypt progenitor phenotype on colorectal cancer cells. Cell *111*, 241–250.

van Es, J.H., van Gijn, M.E., Riccio, O., et al. (2005). Notch/γ-secretase inhibition turns proliferative cells in intestinal crypts and adenomas into goblet cells. Nature *435*, 959–963.

VanDussen, K.L., Carulli, A.J., Keeley, T.M., et al. (2012). Notch signaling modulates proliferation and differentiation of intestinal crypt base columnar stem cells. Development *139*, 488–497.

Velcich, A., Palumbo, L., Selleri, L., et al. (1997). Organization and regulatory aspects of the human intestinal mucin gene (MUC2) locus. J. Biol. Chem. *272*, 7968–7976.

Wang, H., Jin, S., Lu, H., et al. (2017). Expression of survivin, MUC2 and MUC5 in colorectal cancer and their association with clinicopathological characteristics. Oncol. Lett. *14*, 1011–1016.

Watson, P., and Lynch, H.T. (2001). Cancer risk in mismatch repair gene mutation carriers. Fam. Cancer *1*, 57–60.

Yu, T., Chen, X., Lin, T., et al. (2016). KLF4 deletion alters gastric cell lineage and induces MUC2 expression. Cell Death Dis. *7*, e2255.

Zhang, N., Zhang, J., Shuai, L., et al. (2012). Krüppel-like factor 4 negatively regulates β-catenin expression and inhibits the proliferation, invasion and metastasis of gastric cancer. Int. J. Oncol. *40*, 2038–2048.